Chapter 3

A Land Surface Model for Data Assimilation

Selecting a hydrologic model for the land surface data assimilation problem is not an easy task. The model must capture the key physical processes adequately, but at the same time it must be efficient enough to make large-scale optimal estimation computationally feasible. In addition, the variational data assimilation approach also requires a differentiable model. From the variety of models described in the literature, we develop a land surface scheme especially designed for data assimilation purposes. Our land surface scheme is a simple model for moisture and heat transport in the unsaturated soil zone and at the land-atmosphere boundary, together with a Radiative Transfer model relating the soil moisture and temperature to the remotely sensed brightness temperature.

A key assumption is to neglect lateral flow in the unsaturated zone, which is reasonable for terrain with moderate relief and on the spatial scales under consideration. The model domain thus breaks down into a collection of one-dimensional vertical cells or pixels (Figure 4.1). In this Chapter we describe the one-dimensional vertical components of the land surface model and the Radiative Transfer scheme. In Chapter 4 we then describe in detail how these one-dimensional model components can be used in a fully four-dimensional (space and time) land surface data assimilation algorithm.

First, in Section 3.1, we present the one-dimensional model for the moisture and heat dynamics. We use Richards' equation for the moisture transport and the force-restore approximation for the soil temperature. A conceptually similar model of the soil processes has been presented by Ács et al. [1991]. The vegetation model is similar to the Simplified Biosphere Model (SSiB) developed by Xue et al. [1991]. In Section 3.2 we describe the Radiative Transfer (RT) model. The RT model consists of a soil part, including (1) the Dobson mixing model for the wet soil dielectric constant, (2) the Fresnel equations for the soil microwave emissivity, and (3) the gradient RT model or the grey body approximation for the effective soil temperature, and of a vegetation part.

A comprehensive list of all symbols used in the hydrologic model can be found in Appendix B.1. Note the notational convention to label most of the empirical constants in the various parameterizations with κ for scalars and with β for distributed parameters. The constants are superscripted with the variable which is being parameterized and subscripted with a number in case more than one empirical constant is needed.

3.1 Moisture and Heat Transport Model

In this Section we describe a simple one-dimensional model for moisture and heat transport in the unsaturated soil zone and at the land-atmosphere boundary. The moisture dynamics are modeled with Richards' equation, whereas the temperature submodel relies on the force-restore approximation of the heat equation. The dynamics of the moisture and the temperature are coupled via the heat capacity, which depends on the moisture content, and via the evapotranspiration rate/latent heat flux at the land surface. The transport of soil water vapor is entirely neglected. The downward flux of water out of the bottom layer is described by gravitational drainage only. The vegetation submodel is designed after the Simplified Biosphere Model (SSiB) Xue et al. [1991].

3.1.1 Soil Moisture Submodel

Vertical unsaturated flow is described with a modified version of Richards' equation neglecting soil vapor movement and flow due to thermal gradients.

$$\frac{\partial \theta_g}{\partial t} = \frac{\partial}{\partial z} K_u \frac{\partial}{\partial z}(\psi_g + z) - S_g \tag{3.1}$$

The volumetric moisture content is denoted with θ_g $[m^3/m^3]$, the matric head with ψ_g $[m]$, and the unsaturated hydraulic conductivity with K_u $[m/s]$. The sink term S_g $[1/s]$ accounts for root water uptake through transpiration.

At the surface, the boundary condition is the net flux resulting from precipitation falling through the canopy P_t $[m/s]$ and from evaporation from the ground surface E_g $[kg/m^2/s]$

$$q_t = -P_t + E_g/\rho_w \tag{3.2}$$

where ρ_w $[kg/m^3]$ is the density of liquid water. Note that P_t is defined as a positive quantity. The gravity drainage from the bottom layer is given by

$$q_b = -K_u(z_{\text{bottom}}) \tag{3.3}$$

The soil hydraulic properties are parameterized with the model by Clapp and Hornberger [1978]

$$\psi_g = \psi^{\text{CH}} W_g^{-B^{\text{CH}}} \qquad W_g = \left(\frac{\psi_g}{\psi^{\text{CH}}}\right)^{-1/B^{\text{CH}}} \tag{3.4}$$

$$K_u = K_s W_g^{2B^{\text{CH}}+3} \qquad K_u = K_s \left(\frac{\psi_g}{\psi^{\text{CH}}}\right)^{-(2B^{\text{CH}}+3)/B^{\text{CH}}} \tag{3.4a}$$

where the soil wetness or saturation W_g $[-]$ is related to the volumetric soil moisture content θ_g and the porosity θ_s through $W_g = \theta_g/\theta_s$. The hydraulic conductivity at saturation is denoted with K_s. The "matric head at saturation" ψ^{CH} and the parameter B^{CH} are empirical constants.

Recent results on robust solvers for Richards' equation can be found in [Miller et al., 1998]. We discretize Richards' equation following the mass conservative scheme developed by Celia et al. [1990]. For details on the discretized equations see [Simunek et al., 1997]. Here we only introduce the notation for the vertical discretization. The locations of the N_z

vertical nodes are collected into the vector z $[m]$, and the thickness of the layers between the nodes is denoted with Δ $[m]$.

$$\begin{bmatrix} z_1 \\ z_2 \\ \vdots \\ z_{N_z} \end{bmatrix} \qquad \begin{bmatrix} \Delta_1 \\ \Delta_2 \\ \vdots \\ \Delta_{N_z-1} \end{bmatrix} = \begin{bmatrix} z_2 - z_1 \\ z_3 - z_2 \\ \vdots \\ z_{N_z} - z_{N_z-1} \end{bmatrix} \tag{3.5}$$

The vertical coordinate z $[m]$ increases upward and the locations of the bottom and the top nodes are z_1 and z_{N_z}, respectively. Note that the vector Δ has $N_z - 1$ elements.

From the node locations we derive the locations $\bar{z}$ $[m]$ of the mid-points in between the nodes and the thickness $\bar{\Delta}$ $[m]$ of the layers between the mid-points, which is also the thickness of the layers "around" the finite difference nodes.

$$\begin{bmatrix} \bar{z}_1 \\ \bar{z}_2 \\ \vdots \\ \bar{z}_{N_z} \\ \bar{z}_{N_z+1} \end{bmatrix} = \begin{bmatrix} z_1 \\ \frac{z_1+z_2}{2} \\ \vdots \\ \frac{z_{N_z-1}+z_{N_z}}{2} \\ z_{N_z} \end{bmatrix} \qquad \begin{bmatrix} \bar{\Delta}_1 \\ \bar{\Delta}_2 \\ \vdots \\ \bar{\Delta}_{N_z-1} \\ \bar{\Delta}_{N_z} \end{bmatrix} = \begin{bmatrix} \bar{z}_2 - \bar{z}_1 \\ \bar{z}_3 - \bar{z}_2 \\ \vdots \\ \bar{z}_{N_z} - \bar{z}_{N_z-1} \\ \bar{z}_{N_z+1} - \bar{z}_{N_z} \end{bmatrix} = \begin{bmatrix} \frac{\Delta_1}{2} \\ \frac{\Delta_1+\Delta_2}{2} \\ \vdots \\ \frac{\Delta_{N_z-2}+\Delta_{N_z-1}}{2} \\ \frac{\Delta_{N_z-1}}{2} \end{bmatrix} \tag{3.6}$$

It is convenient to define the bottom and the top point as the first and the last mid-points. The vector $\bar{z}$ is thus of length $N_z + 1$, and the vector $\bar{\Delta}$ is of length N_z.

3.1.2 Soil Temperature Submodel

The temperature submodel is based on the force-restore method [Bhumralkar, 1975; Deardroff, 1978; Lin, 1980; Dickinson, 1988; Hu and Islam, 1995]. The force-restore approximation relies on the analytical solution of the heat equation under periodic forcing, which is used to parameterize the almost periodic daily ground heat flux. In this way, a very simple and efficient but reasonably accurate description of the temperature dynamics can be achieved. Only two layers are considered, a surface layer of thickness δ_g $[m]$ at temperature T_g $[K]$, and a deeper layer, which serves as a heat reservoir. The deeper layer is at temperature T_d $[K]$, the depth-average temperature of the soil. The prognostic equation for the temperature T_g in the surface layer is

$$\frac{\partial T_g}{\partial t} = \Gamma_g \left[\Gamma'_g G_g / C_g - (T_g - T_d) \right] \tag{3.7}$$

Here G_g $[W/m^2]$ is the ground heat flux evaluated at the surface, and the coefficients C_g $[J/m^3/K]$, Γ_g $[1/s]$, and Γ'_g $[s/m]$ are discussed below.

At the ground surface, the energy balance (in $[W/m^2]$) consists of the net shortwave radiation R_{gs}^{net}, the net longwave radiation R_{gl}^{net}, the latent heat flux LE_g, and the sensible heat flux H_g. The latent heat of vaporization L $[J/kg]$ is used to convert the mass flux E into a latent heat flux.

$$G_g = R_{gs}^{\text{net}} + R_{gl}^{\text{net}} - LE_g - H_g \tag{3.8}$$

The coefficients Γ_g $[1/s]$ and Γ'_g $[s/m]$ are given by

$$\Gamma_g = \frac{\omega_d}{\alpha_g} \qquad \Gamma'_g = \sqrt{\frac{2}{K_T \omega_d}} = \frac{2}{d_g \omega_d} \tag{3.9}$$

where the coefficient α_g is discussed below, and the damping depth d_g $[m]$ of the daily temperature forcing is

$$d_g = \sqrt{\frac{2\lambda_g}{\omega_d C_g}} = \sqrt{\frac{2K_T}{\omega_d}} \tag{3.10}$$

The angular frequency $\omega_d = 2\pi/86400/s$ enters from the consideration of the analytical formulation with diurnally periodic forcing. The volumetric heat capacity is denoted with C_g $[J/m^3/K]$ and the thermal conductivity with λ_g $[W/m/K]$. Both depend on the soil moisture content and thus vary with time (Section 3.1.7). Lastly, we define thermal diffusivity K_T $[m^2/s]$ as

$$K_T = \frac{\lambda_g}{C_g}. \tag{3.11}$$

As discussed in Section 3.1.7 we use a constant thermal diffusivity, implying that both Γ_g and Γ'_g are constant.

Following [Hu and Islam, 1995], the different versions of the force-restore method can be described by different expressions for the dimensionless coefficient α_g. We will use the version proposed by Hu and Islam [1995], which minimizes the approximation error of the soil temperature at depth δ_g. The computationally efficient polynomial approximation to the optimal α_g is

$$\alpha_g = 1 + \kappa_1^{\alpha_g}(\delta_g/d_g) + \kappa_2^{\alpha_g}(\delta_g/d_g)^2 + \kappa_3^{\alpha_g}(\delta_g/d_g)^3 + \kappa_4^{\alpha_g}(\delta_g/d_g)^4 \tag{3.12}$$

$$\kappa_1^{\alpha_g} = 0.943 \qquad \kappa_2^{\alpha_g} = 0.223 \qquad \kappa_3^{\alpha_g} = 1.68 \cdot 10^{-2} \qquad \kappa_4^{\alpha_g} = -5.27 \cdot 10^{-3}$$

which is valid for $0 \leq \delta_g/d_g \leq 5$. The closed form for greater values of δ_g/d_g can be found in [Hu and Islam, 1995]. If we keep in mind that δ_g is the modeled depth of the surface layer in which the temperature varies diurnally, and that d_g is the damping depth of the forcing, we see that δ_g/d_g should not be far from unity to be consistent. Therefore, the polynomial approximation (3.12) will be appropriate for all practical purposes.

It should be noted that the force-restore versions of Bhumralkar [1975] and of Lin [1980], using $\alpha_g = 1 + 2\delta_g/d_g$ and $\alpha_g = 1 + \delta_g/d_g$, respectively, can be considered special cases of (3.12). They yield similar results for large (Bhumralkar) and small (Lin) values of δ_g/d_g, respectively. For details see [Hu and Islam, 1995].

3.1.3 Vegetation Submodel

The vegetation is modeled with a standard resistance network for the latent and sensible heat fluxes (Figure 3.1).

Canopy Heat Submodel

We assume zero heat capacity for the canopy. The canopy energy balance reads

$$R_{cs}^{\text{net}} + R_{cl}^{\text{net}} - LE_{ct} - LE_{ce} - H_c = 0 \tag{3.13}$$

consisting of the net shortwave radiation R_{cs}^{net}, the net longwave radiation R_{cl}^{net}, the latent heat fluxes LE_{ct} and LE_{ce} from the dry and wet portions of the canopy (canopy transpiration and canopy evaporation), and the sensible heat flux H_c. All fluxes are measured in $[W/m^2]$. This energy balance is solved for the canopy temperature T_c $[K]$.

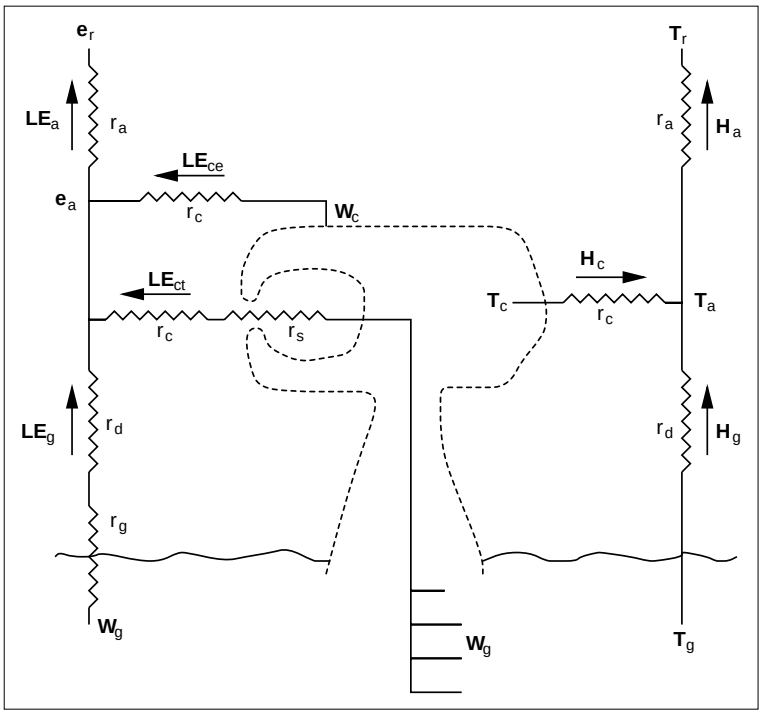

Figure 3.1: Resistance network (after [Xue et al., 1991])

Canopy Water Submodel

If vegetation is present, the canopy intercepts the precipitation. The balance equation for the water W_c $[m]$ stored in the canopy (per unit area) reads

$$\frac{\partial W_c}{\partial t} = P_i - E_{ce}/\rho_w - D_c \tag{3.14}$$

The intercepted flux is denoted with P_i $[m/s]$. The evaporation from the wet canopy is E_{ce} $[kg/m^2/s]$, and D_c $[m/s]$ accounts for dripping off the canopy. We use $D_c = W_c/t_c^{\text{drip}}$, with a typical dripping time t_c^{drip} $[s]$ on the order of $0.5d$ [Thompson and Pollard, 1995].

A simple parameterization for the intercepted precipitation and the evaporation from the wet canopy is

$$\begin{aligned} P_i &= \min\left(f_c P_r, (W_c^{\max} - W_c)/\Delta t\right) \\ E_{ce} &= \min\left(E_{ce}^{\text{pot}}, \rho_w W_c/\Delta t\right) \end{aligned} \tag{3.15}$$

We denote with f_c $[-]$ the fraction of the land surface which is shaded by the canopy. P_r $[m/s]$ is the precipitation at screen (or reference) height z_r $[m]$ as measured by the meteorologic station. (Recall that precipitation is defined as a positive quantity.) E_{ce}^{pot} is the potential evaporation from the wet canopy assuming unlimited water supply. $W_c^{\max}$ $[m]$ is the canopy storage capacity, and Δt $[s]$ is the numerical time step. Equation (3.15) approximately constrains the water stored in the canopy to be nonnegative and less than the storage capacity, $W_c \lesssim W_c^{\max}$. We write the canopy storage capacity as

$$W_c^{\max} = f_c \text{LSAI} \kappa^{W_c} \tag{3.16}$$

where LSAI [−] is the sum of the one-sided leaf area index LAI [−] and the stem area index SAI [−]. The parameter κ^{W_c} $[m]$ is on the order of $\kappa^{W_c} \approx 10^{-4} \ldots 10^{-3} m$ [Abramopoulos et al., 1988]. Finally, we have for the throughfall

$$P_t = P_r + D_c - P_i \tag{3.17}$$

Canopy Air Submodel

We also assume zero heat capacity for the canopy air. The energy balance reads

$$H_a = H_c + H_g \tag{3.18}$$

where H_a $[W/m^2]$ is the overall sensible heat flux to the atmosphere. This energy balance is solved for the temperature of the canopy air T_a $[K]$. The mass balance within the canopy air space is

$$LE_a = LE_g + LE_{ct} + LE_{ce} \tag{3.19}$$

where LE_a $[W/m^2]$ is the overall evapotranspiration to the atmosphere. This mass balance is solved for the vapor pressure of the canopy air e_a $[mb]$.

3.1.4 Radiation Balance

All radiation fluxes are in $[W/m^2]$. The downwelling shortwave and longwave radiation at reference height above the canopy are denoted with R_{rs} and R_{rl}, respectively. For the net fluxes at the ground surface and at the canopy we have [Deardroff, 1978]

$$R_{gs}^{\text{net}} = (1 - f_c)(1 - a_g) R_{rs} \tag{3.20}$$

$$R_{gl}^{\text{net}} = (1 - f_c)\epsilon_g (R_{rl} - \sigma T_g^4) + f_c \frac{\epsilon_c \epsilon_g}{\epsilon_c + \epsilon_g - \epsilon_c \epsilon_g} \sigma (T_c^4 - T_g^4) \tag{3.21}$$

$$R_{cs}^{\text{net}} = f_c (1 - a_c) R_{rs} \tag{3.22}$$

$$R_{cl}^{\text{net}} = f_c \left[\epsilon_c R_{rl} + \frac{\epsilon_c}{\epsilon_c + \epsilon_g - \epsilon_c \epsilon_g} \epsilon_g \sigma T_g^4 - \frac{\epsilon_c + 2\epsilon_g - \epsilon_c \epsilon_g}{\epsilon_c + \epsilon_g - \epsilon_c \epsilon_g} \epsilon_c \sigma T_c^4 \right] \tag{3.23}$$

where a_g, a_c, ϵ_g, and ϵ_c [−] denote the albedos (shortwave) and emissivities (longwave) of the ground and the canopy, respectively, and σ $[W/m^2/K^4]$ is the Stefan-Boltzmann constant.

The parameterization for the ground surface albedo follows [Idso et al., 1975].

$$a_g = \kappa_1^{a_g} - \kappa_2^{a_g} W_g(z_{\text{top}}) \qquad \kappa_1^{a_g} = 0.25 \qquad \kappa_2^{a_g} = 0.125 \tag{3.24}$$

The canopy albedo is on the order of $a_c \approx 0.16 \ldots 0.2$ for grassland and crops.

We compute the downwelling longwave radiation from the air temperature

$$R_{rl} = \epsilon_r \sigma T_r^4 \tag{3.25}$$

and the expressions for the air and the ground surface emissivities are

$$\epsilon_r = \kappa_1^{\epsilon_r} + \kappa_2^{\epsilon_r} e_r \qquad \kappa_1^{\epsilon_r} = 0.74 \qquad \kappa_2^{\epsilon_r} = 0.0049 \tag{3.26}$$

$$\epsilon_g = \kappa_1^{\epsilon_g} + \kappa_2^{\epsilon_g} \theta_g \qquad \kappa_1^{\epsilon_g} = 0.9 \qquad \kappa_2^{\epsilon_g} = 0.18 \tag{3.27}$$

T_r $[K]$ is the atmospheric temperature at screen height, and e_r $[mb]$ is the water vapor pressure at screen height. The formulation of the soil surface emissivity is taken from [Chung and Horton, 1987]. The expression (3.26) for the atmospheric emissivity is known as the *Idso*-formula. For the volumetric soil moisture affecting the long wave radiation we use the top node moisture content $\theta_g = \theta_g(z_{\text{top}})$. The canopy emissivity is on the order of $\epsilon_c \approx 0.95 \ldots 1$.

With both the emissivities for the ground and the canopy being close to unity, we can expand the above equations into series in $(1 - \epsilon_g)$ and $(1 - \epsilon_c)$. Using

$$\epsilon_c + \epsilon_g - \epsilon_c\epsilon_g \equiv 1 - (1 - \epsilon_c)(1 - \epsilon_g)$$

and neglecting terms of second order or higher we get

$$\begin{aligned} R_{gl}^{\text{net}} &= (1 - f_c)\epsilon_g(R_{rl} - \sigma T_g^4) + f_c(\epsilon_c + \epsilon_g - 1)\sigma(T_c^4 - T_g^4) \qquad (3.21a) \\ &= (1 - f_c)\epsilon_g R_{rl} - [\epsilon_g + f_c(\epsilon_c - 1)]\sigma T_g^4 + f_c(\epsilon_c + \epsilon_g - 1)\sigma T_c^4 \\ R_{cl}^{\text{net}} &= f_c\left[\epsilon_c\epsilon_r\sigma T_r^4 + (\epsilon_c + \epsilon_g - 1)\sigma T_g^4 - (2\epsilon_c + \epsilon_g - 1)\sigma T_c^4\right] \qquad (3.23a) \end{aligned}$$

These expressions are used in the model.

3.1.5 Sensible and Latent Heat Fluxes

All sensible and latent heat fluxes are determined with a resistance formulation.[1]

$$H_a = \rho_a c_a \frac{T_a - T_r}{r_a} \qquad (3.28)$$

$$H_g = (1 - f_c)\rho_a c_a \frac{T_g - T_a}{r_d} \qquad (3.29)$$

$$H_c = 2\text{LSAI}\, f_c \rho_a c_a \frac{T_c - T_a}{r_c} \qquad (3.30)$$

$$LE_a = \frac{\rho_a c_a}{\gamma} \frac{(e_a - e_r)}{r_a} \qquad (3.31)$$

$$LE_g = (1 - f_c)\frac{\rho_a c_a}{\gamma} \frac{(e_s(T_g) - e_a)}{r_g + r_d} \qquad (3.32)$$

$$LE_{ce}^{\text{pot}} = f_c f_{ce}\text{LSAI}\frac{\rho_a c_a}{\gamma} \frac{(e_s(T_c) - e_a)}{r_c} \qquad (3.33)$$

$$LE_{ct}^{\text{pot}} = f_c(1 - f_{ce})\text{LAI}\frac{\rho_a c_a}{\gamma} \frac{(e_s(T_c) - e_a)}{r_c + r_s} \qquad (3.34)$$

$$LE_{ct} = \chi_g(W_g) LE_{ct}^{\text{pot}} \qquad (3.35)$$

All latent and sensible heat fluxes are expressed in $[W/m^2]$. The air density is denoted with ρ_a $[kg/m^3]$, the specific heat of air at constant pressure with c_a $[J/kg/K]$, and the psychometric constant with γ $[mb/K]$. The temperature of the canopy is T_c $[K]$. The vapor pressure and the temperature within the canopy air space are e_a $[mb]$ and T_a $[K]$,

[1] Note that we can rewrite the evapotranspiration rate as $E_a = \rho_a(q_a - q_r)/r_a$ by using $\gamma = c_a p_r / L\epsilon$ and $q_r = \epsilon e_r / p_r$, where q_r is the specific humidity, p_r the air pressure, and ϵ the ratio of the gas constants, $\epsilon = R_{\text{dry air}}/R_{\text{vapor}} = 0.622$.

respectively. Furthermore, e_r $[mb]$ and T_r $[K]$ are the vapor pressure and the air temperature at screen or reference height as given by the meteorologic measurements, and $e_s(T)$ $[mb]$ is the saturation vapor pressure at temperature T, calculated by the empirical formula

$$e_s(T) = 6.11 \exp\left\{\frac{17.4(T - T_0)}{T - 34.16}\right\} \tag{3.36}$$

where $T_0 = 273.15K$. Moreover, the fraction of the canopy which is wet and from which water is directly evaporated is denoted with f_{ce} $[-]$ and modeled after [Abramopoulos et al., 1988]

$$f_{ce} = (W_c/W_c^{\max})^{\kappa^{f_{ce}}} \tag{3.37}$$

The resistances r_x and the stress function $\chi_g(W_g)$, which parameterizes water-limited transpiration, are discussed in Section 3.1.6.

3.1.6 Resistances

The resistances can be partitioned into the aerodynamic resistances r_a, r_d, r_c and the surface resistances r_g, r_s. All resistances are measured in $[s/m]$. Water-limited (stressed) transpiration is parameterized with the stress function $\chi_g(W_g)$ $[-]$.

Aerodynamic Resistances

In our scheme we have three aerodynamic resistances: the atmospheric resistance between the canopy air space and the reference level in the atmosphere r_a, the resistance between the leaves and the canopy air space r_c, and the resistance between the soil surface and the canopy air space r_d (Figure 3.1).

The atmospheric resistance for *neutral* conditions (in terms of buoyancy) can be obtained by elimination of the friction velocity u_* $[m/s]$ from the expression (3.39). The friction velocity is a parameter in the logarithmic wind profile (3.38).

$$u_r = \frac{u_*}{K} \ln\left[\frac{z_r - d_c}{z_0}\right] \tag{3.38}$$

$$r_a = \frac{\ln\left[\frac{z_r - d_c}{z_0}\right]}{K u_*} = \frac{\ln^2\left[\frac{z_r - d_c}{z_0}\right]}{K^2 u_r} \tag{3.39}$$

Here, u_r $[m/s]$ is the wind velocity at the reference height z_r $[m]$, $K = 0.4$ is the von Karman constant, and z_0 $[m]$ is the roughness length. The zero displacement height d_c $[m]$ accounts for the geometric effect of vegetation stands. If vegetation of height h_c $[m]$ is present, we use

$$d_c = \kappa^{d_c} h_c \qquad \text{and} \qquad z_0 = \kappa^{z_0} h_c \tag{3.40}$$

with $\kappa^{d_c} = 0.63$ and $\kappa^{z_0} = 0.13$ [Abramopoulos et al., 1988]. Although strictly speaking the zero displacement height vanishes for bare soils, we can still use (3.40) by setting $h_c = z_0/\kappa^{z_0}$ with a roughness length on the order of $z_0 \approx 2.5mm$, which is typical for bare soils. Note that in this case $z_r \gg d_c$ and the error introduced by using (3.40) for bare soil is negligible.

For nonneutral conditions, stability corrections can be taken into account. These corrections are usually parameterized with the gradient Richardson number or the Monin-Obukhov length. Detailed expressions can be found in [Ács et al., 1991]. We will confine ourselves to the assumption of neutral conditions.

For the other two aerodynamic resistances, we use parameterizations from [Sellers and Dorman, 1987].

$$r_c = \frac{\beta^{r_c}}{\sqrt{u_c}} \tag{3.41}$$

$$r_d = \frac{\beta^{r_d}}{u_c} \tag{3.42}$$

The wind speed u_c $[m/s]$ at the canopy top can be obtained from the wind profile (3.38) as

$$u_c = u_r \ln\left[\frac{h_c - d_c}{z_0}\right] \ln^{-1}\left[\frac{z_r - d_c}{z_0}\right] \tag{3.43}$$

Note that a measurement of zero wind speed would lead to numerical problems because the resistances diverge. Such problems are easily overcome by preprocessing and setting all measurements of zero wind speed to a minimum of $0.01m/s$. This is well below the instrument resolution and the error inflicted is negligible.

Surface Resistances

The surface resistance of bare soil r_g $[s/m]$ parameterizes the effect of soil-water limited evaporation. If the upper soil layer is not saturated, the water evaporates at some depth in the soil and must reach the surface through diffusion. We work with the following formulation,

$$r_g = \kappa^{r_g} \exp\left(\beta^{r_g}(W^{r_g} - W_g)\right) \tag{3.44}$$

which depends on three parameters. At saturations $W_g \gtrsim W^{r_g}$ the surface resistance $r_g \lesssim \kappa^{r_g} \equiv 10s/m$ becomes negligible when compared to r_d. The third parameter is the maximum surface resistance $r_g^{\max}$ at zero saturation, which determines $\beta^{r_g} = 1/W^{r_g} \ln(r_g^{\max}/\kappa^{r_g})$. Typical values are $W^{r_g} \approx 0.25 \ldots 0.6$ and $r_g^{\max} \approx 3000 \ldots 7000 s/m$, depending on the texture of the soil in question. Finer soils have higher surface resistances. Figure 3.2 shows the bare soil resistance as a function of the volumetric soil moisture content. Also shown are two formulations by Kondo et al. [1990] and by van de Griend and Owe [1994], which we will not discuss here.

The stomatal resistance r_s $[s/m]$ describes the closure of the plants' stomate due to environmental impacts [Lhomme et al., 1998]. The most important factors determining the transpiration under unstressed conditions (no water limitation) are shortwave (or photosynthetically active) radiation, temperature, and vapor deficit, although some authors believe that the dependence on vapor deficit is an artificial effect. We only retain the dependence of r_s on the shortwave radiation, which essentially shuts off transpiration at night. We use a formulation equivalent to the one in [Dorman and Sellers, 1989]

$$r_s = r_s^{\min} \chi_c(R_{rs}) \tag{3.45}$$

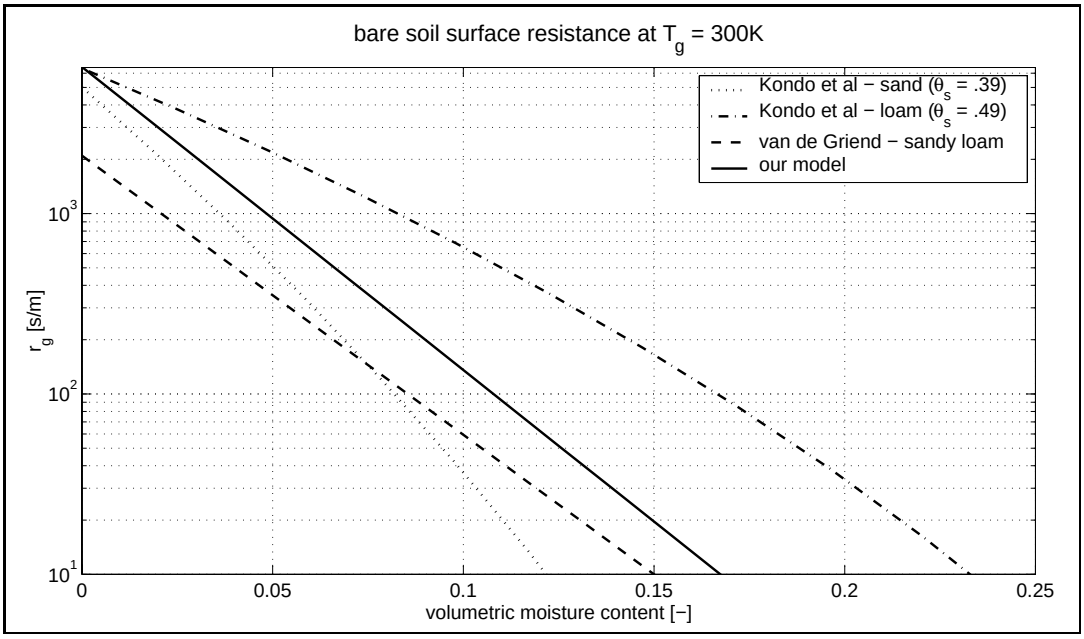

Figure 3.2: Bare soil resistance from (3.44) as a function of the volumetric soil moisture content using $W^{r_g} = 0.6$ and $r_g^{\max} = 6500 s/m$. For comparison, we also show the parameterizations by Kondo et al. [1990] and by van de Griend and Owe [1994].

where

$$\chi_c(R_{rs}) = \begin{cases} \kappa_1^{\chi_c} & R_{rs} < 0 \\ \frac{R_{rs}/\kappa_2^{\chi_c}+1}{R_{rs}/\kappa_2^{\chi_c}+1/\kappa_1^{\chi_c}} & R_{rs} \geqq 0 \end{cases} \tag{3.46}$$

Typical values are $r_s^{\min} \approx 30 \ldots 50 s/m$, $\kappa_1^{\chi_c} \approx 50 \ldots 100$, and $\kappa_2^{\chi_c} \approx 100 \ldots 200 W/m^2$.

The factor $\chi_g(W_g)$ in (3.35) parameterizes the conditions of water-limited transpiration. The total stress is given by the sum over the individual stress terms at the $i = 1 \ldots N_z$ nodes of the vertically discretized soil moisture model.

$$\chi_g(W_g) = \sum_{i=1}^{N_z} \chi_{gi}(W_{gi}) \qquad \chi_{gi}(W_{gi}) = \frac{f_{Ri}}{1 + \psi_{gi}/\psi^{\text{wilt}}} = \frac{f_{Ri}}{1 + \frac{\psi_i^{\text{CH}}}{\psi^{\text{wilt}}} \frac{1}{W_{gi}^{B^{\text{CH}}}}} \tag{3.47}$$

We used (3.4) to obtain the last equality. We denote with ψ^{wilt} $[m]$ the matric head at which the plants start wilting. A typical number is the equivalent of $-15 bar$ [Dickinson et al., 1993]

$$\psi^{\text{wilt}} = -15 bar/\rho_w/g = -153 m \tag{3.48}$$

The acceleration due to gravity is $g = 9.81 m^2/s$. The root distribution factor $f_{Ri} > 0$ measures the root density attributed to node i. We use a simple exponential model for the continuous root density ρ_R $[1/m]$ with maximum density at the top.

$$\rho_R(z) = \left(\frac{1}{d_R}\right) \frac{\exp(\frac{z}{d_R})}{\exp(\frac{z_{N_z}}{d_R}) - \exp(\frac{z_1}{d_R})} \tag{3.49}$$

where $d_R > 0$ $[m]$ is a typical rooting depth. For the root distribution factor f_{Ri} we obtain

$$f_{Ri} = \int_{\bar{z}_i}^{\bar{z}_{i+1}} \rho_R(z)dz = \frac{\exp(\frac{\bar{z}_{i+1}}{d_R}) - \exp(\frac{\bar{z}_i}{d_R})}{\exp(\frac{z_{N_z}}{d_R}) - \exp(\frac{z_1}{d_R})} \tag{3.50}$$

Note that $\rho_R(z)$ is normalized on the interval $[z_1, z_{N_z}]$ and that $\sum_{i=1}^{N_z} f_{Ri} = 1$.

Finally, we can give an expression for the sink term as it appears in the discretized form of Richards' equation (3.1).

$$\bar{\Delta}_i S_{gi} = \chi_{gi}(W_{gi}) E_{ct}^{\text{pot}} / \rho_w \tag{3.51}$$

3.1.7 Thermal Properties of the Soil

The volumetric heat capacity of the surface layer depends on the soil moisture content according to [Simunek et al., 1997]

$$C_g = \rho_{gb} c_g + \theta_g \rho_w c_w \tag{3.52}$$

where c_g $[J/kg/K]$ is the specific heat of the dry soil, ρ_w $[kg/m^3]$ is the density of water, and c_w $[J/kg/K]$ is the specific heat of water. The bulk density of the dry soil ρ_{gb} $[kg/m^3]$ is given by

$$\rho_{gb} = (1 - \theta_s)\rho_g \tag{3.53}$$

where ρ_g $[kg/m^3]$ is the density of the soil particles. A generally accepted number for all soil types is $\rho_g = 2.65 \cdot 10^3 kg/m^3$. For the volumetric moisture content and the porosity which enter the parameterization we choose values averaged over the top layer of thickness δ_g of the force-restore approximation.

Following [Chung and Horton, 1987], the thermal conductivity λ_g $[W/m/K]$ can be parameterized as

$$\lambda_g = \beta_1^{\lambda_g} + \beta_2^{\lambda_g} \theta_g + \beta_3^{\lambda_g} \sqrt{\theta_g} \tag{3.54}$$

The $\beta_i^{\lambda_g}$ depend on the soil type (Table B.5). Figure 3.3 shows the volumetric heat capacity, the thermal conductivity, the thermal diffusivity, and the damping depth as functions of the saturation for three soil types [Chung and Horton, 1987]. We adopt the approximation of a constant heat diffusivity K_T which is justifiable for not too dry conditions, $W_g \gtrsim 0.1$. This is important because for constant K_T the force-restore parameters α_g, d_g, Γ_g, and Γ'_g are also constant and need not be computed at each time step.

3.1.8 Thickness and Number of Soil Layers

In the article by Ács et al. [1991], the thickness of the uppermost soil layer for the moisture submodel is $10cm$, whereas the thickness of the top layer for the temperature submodel is $\delta_g = 2cm$. This disparity is somewhat inconsistent with the model formulation, because the thermal properties of the soil depend on the soil water content. A top moisture layer of $10cm$ thickness can only represent an average moisture value, and it cannot resolve the moisture content of the top $2cm$, which is used in the temperature submodel.

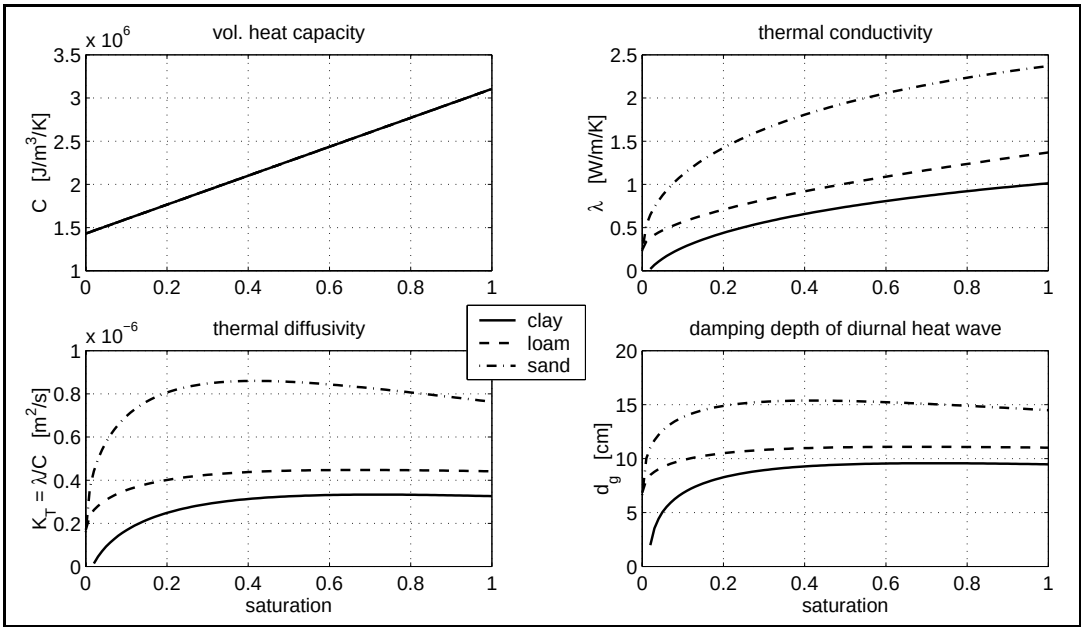

Figure 3.3: Soil thermal properties: volumetric heat capacity (upper left), thermal conductivity (upper right), thermal diffusivity (lower left), and damping depth (lower right) as functions of the saturation W_g. The parameters are $\rho_g = 2.65 \cdot 10^3 kg/m^3$, $\theta_s = 0.4$, $c_g = 900 J/kg/K$.

To be consistent *within* the force-restore approximation, the layer for the temperature T_g should also correspond as much as possible to the layer in which the temperature actually fluctuates. A measure for the thickness δ_g of this layer is the damping depth d_g of the diurnal forcing. Recall from Figure 3.3 that the damping depth d_g varies between $7cm$ and $15cm$ for various soil types and over a wide range of moisture conditions. Similarly, Hu and Islam [1995] cite damping depths d_g that range from $5cm$ (clay) to $20cm$ (rock).

Now note that appreciable errors due to the neglect of higher harmonics can occur in the force-restore method if the upper soil thickness δ_g is less than the damping depth of the diurnal forcing [Hu and Islam, 1995]. This suggests the use of a thicker top soil layer for the temperature submodel. On the other hand, the ground surface temperature T_g from the force-restore method is used in the computation of the boundary fluxes and will also be used for the Radiative Transfer model (Section 3.2). We are therefore interested in the temperature of a shallow layer. Moreover, the diurnal heat wave is much stronger than the higher harmonics, so the errors due to the neglect of higher harmonics should be bearable.

The best overall compromise for moisture and heat transport seems to be a single value of $5cm$ for both the top moisture layer and the δ_g-layer of the force-restore approximation. For the lower layers in the moisture submodel, we use a few layers which reflect the measurement levels of existing time-domain reflectometry (TDR) profile measurement devices. Generally, we work with six layers ranging from 0–$5cm$, 5–$15cm$, 15–$30cm$, 30–$45cm$, 45–$60cm$, and 60–$90cm$. This allows for the assimilation of data from field experiments such as the Southern Great Plains 1997 (SGP97) experiment (Section 5.3.1).

3.2 Radiative Transfer Model

In this Section we describe a model for the Radiative Transfer (RT). It relates the soil moisture and temperature to the remotely sensed radiobrightness temperature T_B, which is a measure of the microwave energy emitted by the soil. In Section 3.2.1 we first describe a model for microwave emission from bare soil, and we then give a complete description in the presence of a vegetation cover in Section 3.2.2.

3.2.1 Microwave Emission from Bare Soil

For microwave emission from bare soil, various coherent and incoherent Radiative Transfer models can be found in the literature [Njoku and Kong, 1977; Wilheit, 1978; Schmugge and Choudhury, 1981; Choudhury et al., 1982; Raju et al., 1995]. Most recently, Galantowicz et al. [1999] discussed and compared several options such as conventional RT, a gradient RT approximation, a grey body approximation, and a coherent model for a stratified medium.

In a non-coherent model, the observed radiobrightness temperature T_B is factored into the microwave emissivity ε_g and the effective soil temperature T_g^{eff}.

$$T_B^{\text{bare}} = \varepsilon_g T_g^{\text{eff}} \tag{3.55}$$

The model then consists of three parts:

1. The wet soil dielectric constant is computed from the dielectric constants of dry soil and water depending on the volumetric soil moisture content (Dobson mixing formula).
2. The microwave emissivity ε_g is obtained from the wet soil dielectric constant (Fresnel equations).
3. The effective temperature T_g^{eff} is determined from the soil temperature profile and possibly the dielectric constant.

In the following subsections, we will discuss each of these steps separately.

Wet Soil Dielectric Constant

The dielectric constant of the wet soil k_g is obtained from the dielectric constants of the dry soil and the soil water, which are evaluated at the microwave frequency of interest. For L-band observations, for instance, the frequency is $\nu_r = 1.4GHz$. Ulaby et al. [1986] present among other models a semi-empirical mixing model which makes use of soil texture information in order to account for the bound water contribution in an aggregate way. We call their model the Dobson mixing model because it is an improved version of the semi-empirical mixing model presented by Dobson et al. [1985]. In particular, the model for the wet soil dielectric constant reads

$$k_g = \left\{ 1 + (1 - \overline{\theta_s})(k_{gd}^{\kappa_1^{k_g}} - 1) + \overline{\theta_g}^{\beta^{k_g}} (k_w^{\kappa_1^{k_g}} - 1) \right\}^{(1/\kappa_1^{k_g})} \tag{3.56}$$

with

$$\beta^{k_g} = \kappa_2^{k_g} - \kappa_3^{k_g} f_S - \kappa_4^{k_g} f_C \tag{3.57}$$

where f_S $[-]$ and f_C $[-]$ are the sand and clay fractions of the soil in question. The $\kappa_i^{k_g}$ are empirical constants. Their values can be found in Table B.7. The porosity $\overline{\theta_s}$ and the volumetric moisture content $\overline{\theta_g}$ are appropriate averages over depth (Section 3.2.1). For L-band observations, Galantowicz et al. [1999] used averaging depths of $1.5cm$ and $2cm$ for gradient RT and grey body RT, respectively (Section 3.2.1). In our coarse discretization (Section 3.1.8) we best use an average moisture content and an average porosity over the top layer.

The dielectric constant of the dry soil k_{gd} depends only very weakly on the density of the soil particles. A good approximation for all soil types is [Dobson et al., 1985]

$$k_{gd} = 4.67 \tag{3.58}$$

The dielectric constant of water k_w $[-]$ at the microwave frequency ν_r $[Hz]$ and temperature T $[K]$ is determined with a Debye model [Ulaby et al., 1986].

$$k_w = k_{w\infty} + \frac{(k_{w0} - k_{w\infty})}{1 + (2\pi\nu_r\tau_w)^2}\left(1 + i \cdot 2\pi\nu_r\tau_w\right) \tag{3.59}$$

where $k_{w\infty} = 4.9$ is the high frequency limit of k_w. The static limit k_{w0} $[-]$ as well as the relaxation time of water τ_w $[s]$ are given by Taylor series expansions.

$$k_{w0} = \kappa_1^{k_{w0}} + \kappa_2^{k_{w0}}(T - T_0) + \kappa_3^{k_{w0}}(T - T_0)^2 + \kappa_4^{k_{w0}}(T - T_0)^3 \tag{3.60}$$

$$\tau_w = \frac{1}{2\pi}\left\{\kappa_1^{\tau_w} + \kappa_2^{\tau_w}(T - T_0) + \kappa_3^{\tau_w}(T - T_0)^2 + \kappa_4^{\tau_w}(T - T_0)^3\right\} \tag{3.61}$$

The coefficients $\kappa_i^{\tau_w}$ and $\kappa_i^{k_{w0}}$ are listed in Table B.7. The reference temperature is $T_0 = 273.15K$. We choose for the temperature $T = T_g$ from the force-restore approximation (Section 3.2.1).

Figure 3.4 shows the dependence of the wet soil dielectric constant on soil moisture for the five soil types discussed by Dobson et al. [1985] together with the wet soil dielectric constant derived from two dielectric mixing models presented by Birchak et al. [1974], which we will not discuss here. Figure 3.5 shows the dielectric constant of water at frequency $\nu_r = 1.4GHz$ as a function of temperature. Note that the temperature effect is of the same order as the texture effect (Figure 3.4).

Microwave Emissivity

The microwave emissivity for a smooth soil surface is readily obtained from the Fresnel equations. The microwave emissivities of the soil for horizontal polarization $\varepsilon_{gh}^{\text{smooth}}$ and for vertical polarization $\varepsilon_{gv}^{\text{smooth}}$ are for a look-angle ϕ_r from nadir (in air)

$$\varepsilon_{gh}^{\text{smooth}} = 1 - \left|\frac{k_g\cos\phi_r - \sqrt{k_g - \sin^2\phi_r}}{k_g\cos\phi_r + \sqrt{k_g - \sin^2\phi_r}}\right|^2 \tag{3.62}$$

$$\varepsilon_{gv}^{\text{smooth}} = 1 - \left|\frac{\cos\phi_r - \sqrt{k_g - \sin^2\phi_r}}{\cos\phi_r + \sqrt{k_g - \sin^2\phi_r}}\right|^2 \tag{3.63}$$

$$\varepsilon_{gn}^{\text{smooth}} = 1 - \left|\frac{\sqrt{k_g} - 1}{\sqrt{k_g} + 1}\right|^2 \tag{3.64}$$

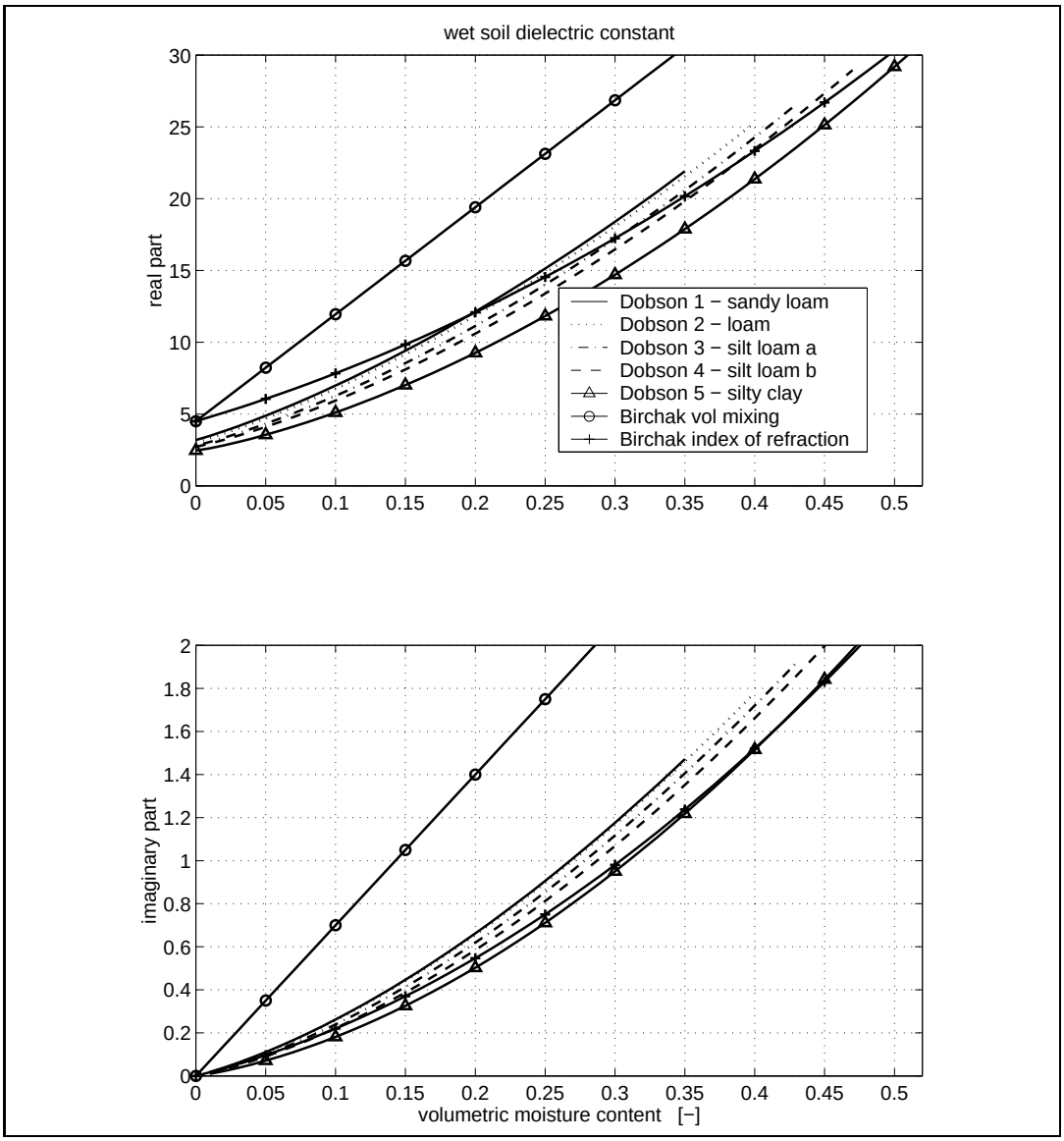

Figure 3.4: Wet soil dielectric constant for the five soil types discussed by Dobson et al. [1985] together with the wet soil dielectric constant derived from two dielectric mixing models presented by Birchak et al. [1974] at $T_g = 300K$ and $1.4GHz$ as a function of the volumetric moisture content.

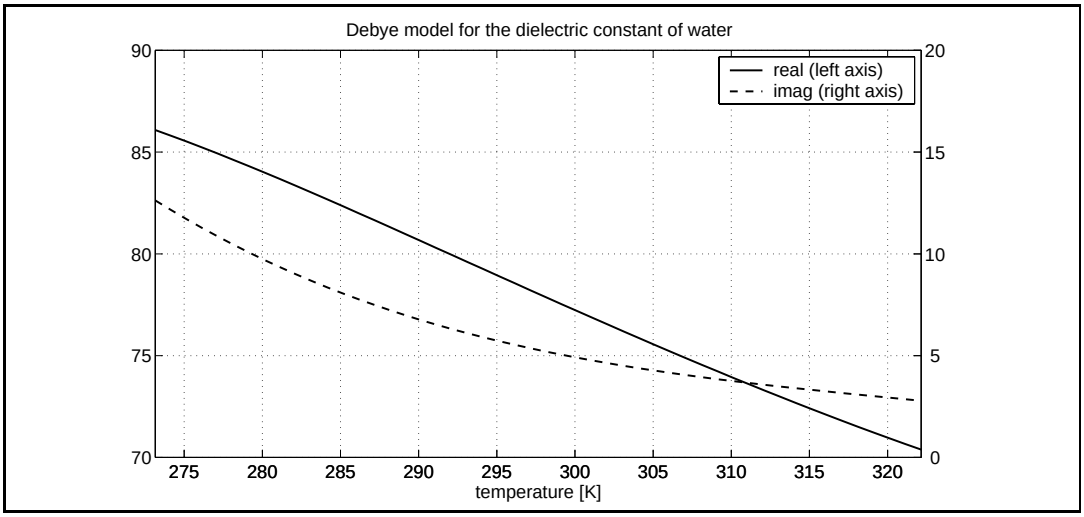

Figure 3.5: Dielectric constant of water k_w at frequency $\nu_r = 1.4GHz$ as a function of temperature T $[K]$.

The last equation shows the microwave emissivity for incidence from nadir ($\phi_r = 0$). For microwave frequencies and look-angles $\phi_r \approx 10^\circ$ the nadir incidence formula is a very good approximation for both the horizontal and vertical polarization formulae. Note also that strictly speaking the emissivities are zero if the look-angle ϕ_r is larger than the critical angle at which total reflection occurs. We do not consider this case and assume that ϕ_r is small enough.

Figure 3.6 shows the microwave emissivities for the five soil types discussed by Dobson et al. [1985] together with the emissivities derived from two dielectric mixing models presented by Birchak et al. [1974], which we will not discuss here.

Roughness Effects The previous discussion assumed the soil surface to be smooth, but this is rarely the case in nature. Roughness effects can be taken into account with a simple one-parameter model developed by Choudhury et al. [1979]. The overall effect of roughness is to increase the emissivity, that is to decrease the reflectivity. In the model, the reflectivity is modified by an exponential term including the roughness parameter β^{ε_g} $[-]$

$$\varepsilon_{gp} = 1 - (1 - \varepsilon_{gp}^{\text{smooth}}) \exp(-\beta^{\varepsilon_g} \cos^2 \phi_r) \tag{3.65}$$

Using (3.62), the emissivity for incidence from nadir ($\phi_r = 0$) is

$$\varepsilon_{gn} = 1 - \left| \frac{\sqrt{k_g} - 1}{\sqrt{k_g} + 1} \right|^2 \exp(-\beta^{\varepsilon_g}) \tag{3.66}$$

Effective Temperature

The effective temperature generally depends on the soil temperature and moisture profiles, where the moisture profile enters primarily through the dielectric constant. For our objectives, there are primarily two choices of models: the gradient RT model and the grey body RT approximation, which are both non-coherent models.

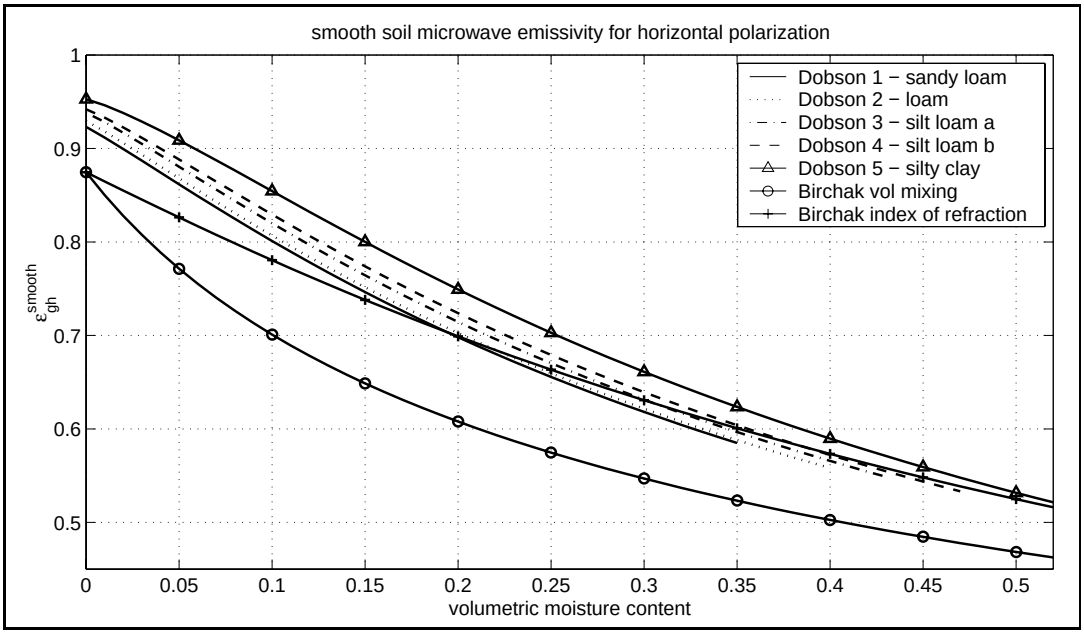

Figure 3.6: Microwave emissivities $\varepsilon_{gh}^{\text{smooth}}$ for horizontal polarization ($\phi_r = 10°$) for the five different soils in [Dobson et al., 1985] and for two models presented by Birchak et al. [1974] at $T_g = 300K$.

Gradient RT Model In the gradient RT model, the effective temperature is given by

$$T_g^{\text{eff}} = T(z_{\text{grad}}) - \frac{(1 - c_{\text{grad}})\cos\phi_g}{\alpha_e} \left.\frac{dT}{dz}\right|_{z_{\text{grad}}} \tag{3.67}$$

where

$$\alpha_e = \frac{4\pi\nu_r}{c_{\text{light}}} \text{Im}\sqrt{k_g}$$

is the attenuation coefficient and

$$z_{\text{grad}} = -\frac{c_{\text{grad}}\cos\phi_g}{\alpha_e}$$

is an effective depth for the gradient RT model. The in-soil propagation angle ϕ_g is obtained from Snellius' law.

$$\phi_g = \arcsin(\sin\phi_r/\sqrt{k_g}) \tag{3.68}$$

The speed of light is $c_{\text{light}} = 3 \cdot 10^8 m/s$, and finally, c_{grad} is a gradient RT parameter. Galantowicz et al. [1999] use $c_{\text{grad}} = 1.03$. Figure 3.7 shows the gradient RT effective depth z_{grad} for the same soils and models as Figure 3.6.

Grey Body RT Model In a grey body approximation, one simply uses

$$T_g^{\text{eff}} = T(z_{\text{grey}}) \tag{3.69}$$

The parameter z_{grey} determines the depth at which the temperature is evaluated. For L-band observations, Galantowicz et al. [1999] use a depth of $z_{\text{grey}} = 1.5cm$.

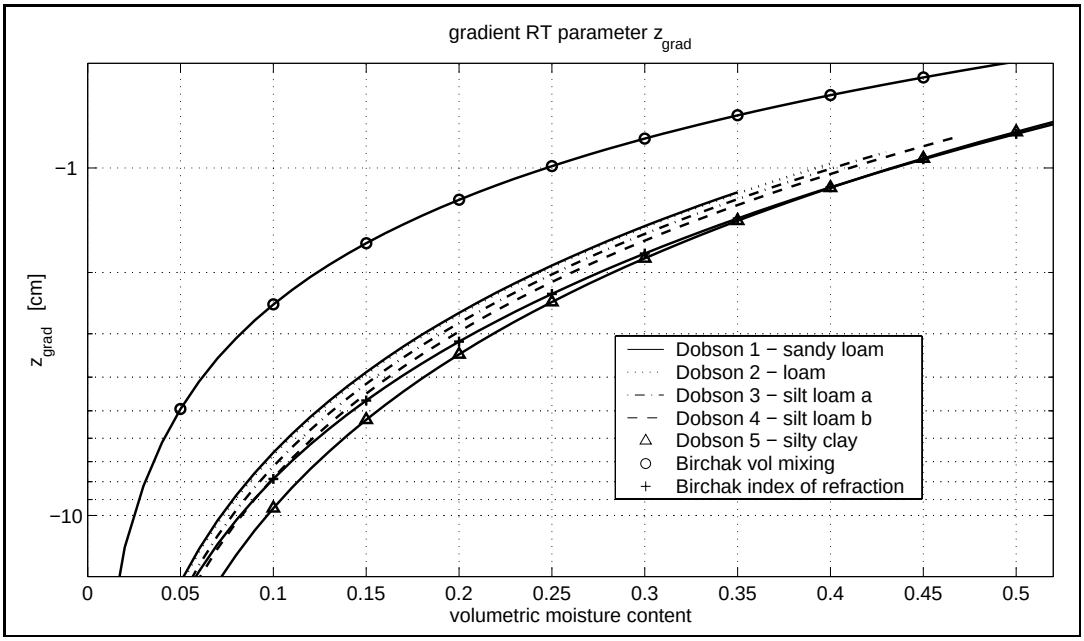

Figure 3.7: Gradient RT effective depth z_{grad} for the five different soils in [Dobson et al., 1985] and for two models presented by Birchak et al. [1974].

Choice of a Model The appropriate choice of the RT model depends on the damping depth d_g and the resulting discretization δ_g chosen in the force-restore approximation of the heat equation (Section 3.1.2). Recall that the damping depth d_g describes the penetration depth of the diurnal heat wave, whereas z_{grey} and z_{grad} relate to the penetration depths of the microwaves.

According to Galantowicz et al. [1999], the gradient RT model is superior to the grey body approximation over the full diurnal cycle if the parameters are calibrated with daytime data. However, the force-restore model provides an approximate temperature gradient only at a depth $d_g \approx \delta_g$. Now recall from Figure 3.7 that for all soils and most moisture conditions, $z_{\text{grad}} \lesssim 5cm$. Compared to the typical damping depth and discretization $d_g \gtrsim \delta_g \approx 5cm$ (Section 3.1.2), we see that the use of the gradient RT model might be inappropriate. From the force-restore method, we cannot get the temperature gradient we need in the gradient RT approximation. In summary, we therefore use the grey body RT approximation with $T_g^{\text{eff}} = T_g$.

3.2.2 Microwave Emission in the Presence of a Canopy

If vegetation is present, the radiation observed by the instrument is given by

$$\begin{aligned} T_B =& (1 - f_c)\varepsilon_g T_g^{\text{eff}} \\ &+ f_c \left[\varepsilon_g T_g^{\text{eff}} \alpha_c + (1 - \alpha_c) T_c + (1 - \alpha_c) T_c (1 - \varepsilon_g) \alpha_c\right] \end{aligned} \tag{3.70}$$

The first term (proportional to $(1 - f_c)$) is the direct microwave emission from the bare or unshaded portion of the soil. The other three terms (proportional to f_c) are

- emission from the soil attenuated by the canopy,

Vegetation type	$\delta_c \cos\phi_r$ $[-]$	W_v $[kg/m^2]$	β^{δ_c} $[m^2/kg]$
Corn	-	-	0.115
Corn	0.452	4.0	0.113
Corn	0.163	1.2	0.133
Corn	0.611	6.0	0.102
Soybean	-	-	0.086
Soybean	0.087	1.0	0.087
Sorghum	0.613	5.4	0.105
Winter Rye	0.080	0.7	0.114
Short Grass	0.093	0.3	0.300
Tall Grass	0.288	0.4	0.720
Tall Grass	-	0.5	0.150
Rangeland, Pasture	-	-	0.098

Table 3.1: L-band (wavelength $21cm$) parameters for the canopy transmissivity [Jackson and Schmugge, 1991].

- direct (upward) emission from the canopy (neglecting canopy reflection, that is emission equals absorption equals one-minus-transmission),
- ground surface reflection of emission from the canopy and attenuated by the canopy.

The model follows [Ulaby et al., 1986] (p. 1552), where we neglected the scattering albedo [Jackson and Schmugge, 1991]. We can rewrite (3.70) as

$$\begin{aligned} T_B &= \left[1 - f_c(1-\alpha_c)\right] \varepsilon_g T_g^{\text{eff}} + f_c T_c \left[(1-\alpha_c)(1+(1-\varepsilon_g)\alpha_c)\right] \\ &= \left\{ \left[1 - f_c(1-\alpha_c)\right] T_g^{\text{eff}} - \left[f_c \alpha_c (1-\alpha_c)\right] T_c \right\} \varepsilon_g + f_c(1-\alpha_c^2) T_c \end{aligned} \tag{3.70a}$$

The canopy microwave attenuation α_c $[-]$ depends on the canopy optical thickness δ_c $[-]$.

$$\alpha_c = \exp(-\delta_c) \tag{3.71}$$

The optical thickness is parameterized as

$$\delta_c = \beta^{\delta_c} W_v / \cos\phi_r \tag{3.72}$$

where W_v $[kg/m^2]$ is the vegetation water content, and ϕ_r is the look-angle from nadir. For the L-band ($\nu_r = 1.4GHz$), some of the parameters given by Jackson and Schmugge [1991] can be found in Table 3.1.